 

PACS numbers: 42.55.Px; 42.60.Da; 42.60.Jf
DOI: 10.1070/QE2010v040n07ABEH014340

# Catastrophic optical degradation of the output facet of high-power single-transverse-mode diode lasers. 1. Physical model

D.R. Miftakhutdinov, A.P. Bogatov, A.E. Drakin

***Abstract*. The physical model of catastrophic optical degradation (COD) of the output facet of high-power single-transverse-mode diode lasers is developed. The model excels other models both in completeness of the physical analysis of the processes leading to COD and in allowance for design feature of lasers used to increase the COD threshold – protective coating of the output facet and current limitations near it.**

***Keywords***: *high-power diode lasers, catastrophic optical degradation.*

## 1. Introduction

One of the main problems preventing an increase in the optical power of diode lasers is catastrophic optical degradation (COD) of the output facet of a laser when some critical density of the optical beam is achieved. This phenomenon occurs, as a rule, while heating the output facet, due to absorption of intracavity radiation by a near-surface region, to the melting temperature, followed by irreversible degradation of the output facet material. Even now, despite many works in this field (see, for example, review [1] and references therein), the COD mechanism cannot be treated conclusively elucidated. Understanding the COD processes requires their simulation and comparison of the obtained results with the data of experimental measurements.

Using simulation, we can optimise the laser design for increasing the COD threshold by decreasing the number of long and expensive experiments. In this case, increasing the COD threshold will make it possible both to obtain a higher output power and (at the same power) to increase the mean time between failures.

One of the first models, in which the COD physics is clearly presented, was Henry's model [2] proposed already in 1979. However, this model can be hardly treated satisfactory because it leads to the results, which are, generally speaking, not consistent (at times even qualitatively) with the experiment. Henry's model was later developed in other papers [3 – 5] which, however, retained its main drawbacks and explained qualitatively only some aspects of the COD phenomenon. Later, there appeared new models [6 – 11], which self-consistently take into account thermal and laser relations, but these models did not provide a complete COD description because they do not take into account all the physical mechanisms responsible for this phenomenon.

In this paper, we have developed a model, which, first, includes all the mechanisms known to us, affecting one way or the other the COD threshold. Second, the model makes it possible to perform calculations for lasers with a more complex design than that used previously. In particular, these are the lasers with a dielectric coating of output facets as well as the lasers blocking the injection current near the output mirror (nonabsorbing mirror). These designs are especially urgent for high-power lasers. In addition, the model under study allows the analysis of the COD development dynamics.

## 2. Model

The model is based on two self-consistent coupled problems: the three-dimensional thermal problem and the quasi-three-dimensional laser problem.

An important feature of the COD is its threshold character, which is the result of the positive feedback considered in many earlier works (see, for example, [7, 8, 11 – 13]). Several processes caused by the temperature rise (decrease in thermal conductivity, growth of different types of optical absorption, increase in the nonradiative recombination) simultaneously play the role in the formation of the positive feedback. They all lead to an additional heat release and, thus, to a higher temperature rise. At the same time, there exists a negative feedback, which mainly takes place due to the laser power fall (and, hence, a decrease in the heat release due to absorption) when heating the volume or some volume of the laser cavity.

With increasing the pump current, two possibilities can be realised. In the first one, the positive feedback dominates and, starting with some laser power level, becomes sufficient for the instability to appear, which is followed by an avalanche temperature rise up to the onset of the laser material melting. After it, the irreversible COD takes place. The second possibility is realised when the negative feedback dominates. In this case, the increase in the optical power with increasing the current slows down and even achieves saturation, and then monotonically decreases. In foreign literature this process is known as a rollover of the light – current characteristic (see, for example, [14]). As a rule, it is

**D.R. Miftakhutdinov, A.P. Bogatov, A.E. Drakin** P.N. Lebedev Physics Institute, Russian Academy of Sciences, Leninsky prosp. 53, 119991 Moscow, Russia; e-mail: mifta@sci.lebedev.ru

Received 26 April 2010
*Kvantovaya Elektronika* **40** (7) 583 – 588 (2010)
Translated by I.A. Ulitkin

reversible and does not lead to irreversible degradation of the laser at least during one experiment. In this case, the maximal power is limited not by the COD but by other physical reasons, which are beyond the scope of this paper.

Nevertheless, because the negative feedback exists and is related to the thermal changes in the laser parameters, it is necessary to consider self-consistently the thermal and laser problems.

## 3. Thermal problem

The heat conduction equation in our model has the form:

$$C(\boldsymbol{r})\,\frac{\partial T}{\partial t} = \mathrm{div}[\kappa(\boldsymbol{r},T)\mathrm{grad}T] + F(\boldsymbol{r},T), \tag{1}$$

where $C$ and $\kappa$ are the heat capacity and heat conductivity for different calculation domains (Fig. 1), and $F(\boldsymbol{r},T)$ is the power density of thermal sources, depending on the coordinates $\boldsymbol{r}=(x,y,z)$ and temperature; below these sources will be considered in detail.

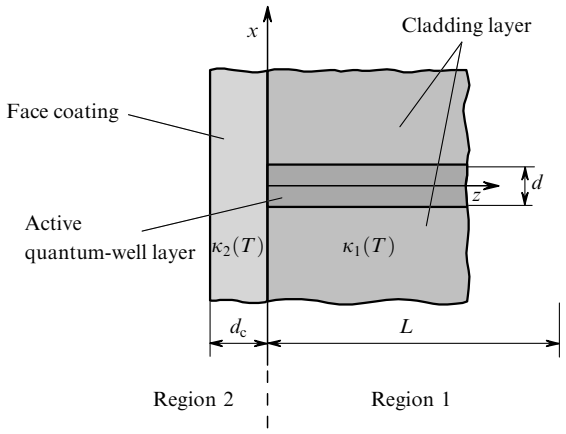


**Figure 1.** Calculation region.

Equation (1) is solved in two regions: in the laser cavity (region 1) and in the coating of its output facet (region 2) of thickness $d_c$. We consider a simplified heterostructure (symmetric with respect to the plane $x=0$) consisting of three plane layers (quantum-dimensional active and two cladding layers 25 μm in thickness). In fact, a real laser structure is much more complicated and can consist of more than ten layers but we believe that this simplification does not influence significantly the calculation results. Real expressions for the thicknesses of the layers and their heat conductivities are such that it is possible to replace these layers by two effective layers with some averaged value of the heat conductivity, the layers being located at both sides of the active region.

For the heat conductivity $\kappa(T)$, we can find in the literature the empiric expression

$$\kappa(T) = \kappa_0(\tilde{T}/T)^{n_\kappa}. \tag{2}$$

Here, the exponent $n_\kappa$ lies in the region $1.2 \leqslant n_\kappa \leqslant 1.55$ (see, for example, [15] and references therein) for different materials and the temperature range. Hereafter, $\tilde{T}$ is the surrounding temperature. In our model we use the expression $n_\kappa(T) = n_\kappa^0 + (\partial n_\kappa/\partial T)(T-\tilde{T})$. It is valid for the anomalously large temperature range (from room temperature to melting temperature) when selecting the corresponding values of $n_\kappa^0$ and $\partial n_\kappa/\partial T$. We used the values obtained by fitting the data of paper [16].

The model takes into account six thermal sources:

$$F(x,y,z,T) = \sum_{i=1}^{6} F_i(x,y,z,T). \tag{3}$$

Let us consider these sources.

(i) Heat release caused by thermalisation of the injected carriers in the active region ($F_1$):

$$F_1 = \theta\left(\frac{d}{2}-|x|\right)\exp\left(-\frac{\pi y^2}{w^2}\right)\phi(z)\,\frac{j}{d}\left[V_{\mathrm{p-n}}-\frac{\hbar\omega}{e}\right]. \tag{4}$$

Here, $\theta$ is the Heaviside function; $d$ and $w$ are the thickness and width of the active region; $\phi(z)$ is the dimensionless function characterising nonuniform excitation of the active medium due to the current isolation of the region near the output mirror with the isolated segment length $a$. At $a=0$ (current limitations are absent), the function $\phi(z)\equiv 1$ and at $a \gg \lambda$ ($\lambda$ is the carrier diffusion length along the $z$ axis), it is approximated by the expression

$$\phi(z) = \left[1+\exp\left(-\frac{z-a}{\lambda}\right)\right]^{-1}. \tag{5}$$

This heat source is formed due to the fact that non-equilibrium carriers with the current density $j$ are injected through the p–n transition with the voltage $V_{\mathrm{p-n}}$, exceeding the laser photon energy $\hbar\omega$. Because of carrier thermalisation (electrons and holes), heat whose power density is equal to the product of the current density by the difference $V_{\mathrm{p-n}}-\hbar\omega/e$ is released. Assuming the heat release in the active region to be uniform over its thickness, we obtain expression (4). In the model we consider the current density to be spatially homogeneous (except for the region of current limitation near the output facet).

(ii) Thermalisation of the carriers produced due to the resonance absorption of laser radiation ($F_2$):

$$F_2 = -\theta\left(\frac{d}{2}-|x|\right)g(y,z,T)I(x,y,z)\,\frac{\hbar\omega - E_{\mathrm{a}}^{\mathrm{g}}(T)}{\hbar\omega},$$

$$\text{for} \quad g(y,z) < 0 \tag{6}$$

$$F_2 = 0 \quad \text{for} \quad g(y,z) \geqslant 0.$$

Here, $g(y,z,T)$ are the material gain (resonance absorption); $I(x,y,z)$ is the current density of the optical power in the active layer; $E_{\mathrm{a}}^{\mathrm{g}}(T)$ is the bandgap width in the active region. The specific expression for $g$ is presented below [see (22)]. The temperature dependence of the bandgap width is assumed linear, which corresponds to experimental data (see, for example, [17] and references therein):

$$E_{\mathrm{a}}^{\mathrm{g}} = E_{\mathrm{a}}^{\mathrm{g}}(\tilde{T}) + \frac{\partial E_{\mathrm{a}}^{\mathrm{g}}}{\partial T}\,(T-\tilde{T}). \tag{7}$$

As is known, heating the active region leads to a decrease in the bandgap width. In strongly heated regions, there appears absorption caused by the fact that the active region width becomes markedly smaller then $\hbar\omega$. Due to this absorption, electron–hole pairs are produced, whose ther-

malisation leads to an additional heat release. The last factor in the expression is explained by the fact that after the electron–hole pair energy falls approximately down the bandgap width level due to fast intraband relaxation, this pair recombines with photon emission (or recombination is nonradiative, which is taken into account below).

(iii) Heat release due to nonradiative recombination ($F_3$)

$$F_3 = \theta\left(\frac{d}{2} - |x|\right)\frac{N(y,z)}{\tau_{\mathrm{nr}}(T)}\,E_{\mathrm{a}}^{\mathrm{g}}(T). \tag{8}$$

All the possible processes of nonradiative relaxation of the carriers with the concentration $N(y,z)$, independently of their origin (Auger recombination, multiphoton recombination, etc.), are described by one term with the characteristic recombination time $\tau_{\mathrm{nr}}$. We are not interested in the details of these processes; suffice it to say that the energy of electron–hole pairs in these processes is finally released as heat. We equate this energy, as in the previous case, with the bandgap width by neglecting the energy distribution of nonequilibrium carriers. The account for this distribution yields a small correction lying outside the model accuracy.

The nonradiative recombination time can be conveniently expressed by the spontaneous radiative recombination $\tau$, which is the only characteristic scale:

$$\frac{1}{\tau_{\mathrm{nr}}} = \frac{1}{\tau}\exp\left(\frac{T - T_{\mathrm{b}}}{T_{\tau}}\right), \tag{9}$$

where $T_{\mathrm{b}}$ is the temperature at which the rates of radiative and nonradiative recombinations coincide and $T_{\tau}$ is the temperature characterising the increase in the nonradiative recombination with heating. These two temperatures depend both on the chemical composition of the active medium and on the quality of its manufacturing. In our paper, we use typical values of these parameters known from literature (see, for example, [18, 19]).

(iv) Heat release caused by absorption near the output facet ($F_4$).

The mechanism of this heat release is caused by a change in the optical properties of the material due to the crystal defects near the laser facet. The origin of such defects is the damage of the crystal lattice as a result of broken electronic bonds of atoms on the lattice surface, leading to significant distortions of its band structure. Apart from this, we deal with adsorption of atoms from the surroundings, followed by their diffusion inside the crystal. These violations in the laser operation serve as a seed for more complex photochemical, recombination, and diffusion processes proceeding near the facet surface and resulting in the accumulation of different crystal defects in this region, for example, vacancies, interstitial atoms, dislocations as well as local deviation from stoichiometry.

Many experimental studies (see, for example, [12, 20]) showed that the region of the broken crystal lattice expands with time inside the crystal, the rate of this expansion increasing markedly with increasing the power of the operating laser.

The change in the optical properties of the near-surface layer is simulated by introducing absorption

$$\alpha^{\deg} = \alpha_0^{\deg}\exp\left(-\frac{z}{z_0}\right), \tag{10}$$

where $\alpha_0^{\deg}$ is the absorption near the surface; $z_0$ is the characteristic depth of defect penetration. It is clear that during the laser operation the parameter $z_0$ increases due to expansion of the defect region inside the crystal, which was mention above. The parameter $\alpha_0^{\deg}$ can also change. Any reliable calculations for $\alpha_0^{\deg}$ and $z_0$ are absent now. For this reason, in our model these parameters varied in the regions $2\times10^4 \leqslant \alpha_0^{\deg} \leqslant 5\times10^5$ см$^{-1}$ and $0 < z_0 \leqslant 3$ μm. Because the absorbing defect region appears on the surface of both the active region and the cladding layers, we reduce, for convenience of further calculations, $\alpha_0^{\deg}$ and $z_0$ to some effective values typical only of the active region.

Heat release caused by this absorption is given by the expression

$$F_4 = \theta\left(\frac{d}{2} - |x|\right)I(x,y,z)\alpha^{\deg}(z). \tag{11}$$

Note here the protective role of the output facet coating. Because the main reason for the appearance of absorption is damaged electronic bonds, after depositing an optimally chosen protective coating, whose atoms saturate these bonds, on a rather clean cleaved facet, we can expect a decrease in the number of defects and, thus, a decrease in absorption $\alpha_0^{\deg}$ and degradation depth $z_0$.

It is obvious that the defects develop not only on the output but also on the rear facet; however, we do not take into account these processes because the radiation flux density of a high-power laser near the rear facet is significantly smaller than near the output mirror. Therefore, the COD will likely occur due to the damage of the output facet.

(v) Heat release due to near-surface nonradiative recombination ($F_5$).

As was noted above, the electron spectrum near the crystal surface differs substantially from that within its volume. The appearance of new states can favour the emergence of nonradiative electronic transitions transferring the energy of the electron–hole pair [$\sim E_{\mathrm{a}}^{\mathrm{g}}(T)$] into thermal energy. For the nonradiative surface recombination rate $R$ we used in the model the relation often used in the literature (see, for example, [21])

$$R = QN(y,z). \tag{12}$$

The coefficient $Q$ lies, as a rule [22], in the range $7\times10^4 - 2\times10^6$ cm s$^{-1}$. Such a wide spread of values is caused not by the low accuracy of $Q$ measurements but by the different quality of the surfaces of various samples due to the differences in the technologies and processing history. Taking (12) into account, the thermal source has the form

$$F_5 = \theta\left(\frac{d}{2} - |x|\right)\delta(z)QN(y,z)E_{\mathrm{a}}^{\mathrm{g}}(T), \tag{13}$$

where $\delta(z)$ is the delta function indicating that the sources are on the surface $z = 0$.

(vi) Heat release due to optical absorption in heated cladding layers ($F_6$).

Most papers devoted to optical damage of the output facet agree that optical absorption is possible only in active layers. In barrier and cladding layers absorption is usually assumed absent because the energy of the laser radiation quantum is significantly smaller than the bandgap width. Even taking into account the temperature decrease in the

bandgap width, the photon energy does not fall into the region of fundamental absorption.

In this paper we consider a quite different mechanism. From our point of view, the physical reason behind this absorption is the 'tails' of electronic states extending inside the band gap. There exists an empirical law known as Urbach's rule [23] according to which this absorption decreases under the exponential law with decreasing the quantum energy inside the band gap. The authors of paper [24] measured this absorption for GaAs in the temperature range 52–632 °C; the obtained experimental data for long-wavelength absorption in cladding layers $\alpha^{\mathrm{cl}}$ were interpolated by the relation

$$\alpha^{\mathrm{cl}}(T) = \alpha_0^{\mathrm{cl}} \exp\left(\frac{\hbar\omega - E_{\mathrm{eff}}(T)}{\Lambda(T)}\right), \tag{14}$$

where

$$E_{\mathrm{eff}}(T) = E_{\mathrm{eff}}^0 - pk\theta[\exp(\theta_{\mathrm{E}}/T) - 1]^{-1};$$
$$\Lambda(T) = qk\theta_{\mathrm{E}}\{(1+\Lambda)/2 + [\exp(\theta_{\mathrm{E}}/T) - 1]^{-1}\}; \tag{15}$$

$p$ and $q$ are dimensionless constants; $k$ is the Boltzmann constant; $\theta_{\mathrm{E}}$ is the Einstein temperature; $E_{\mathrm{eff}}^0 = E_{\mathrm{eff}}(T=0)$ is the effective energy of interband transition with absorption quantity $\alpha^{\mathrm{cl}}$; $\Lambda$ is the disorder parameter; $\Lambda$ is the effective absorption band in cladding layers.

The physical reason for the emergence of electronic states responsible for long-wavelength absorption inside the band gap is the fluctuations of the crystal potential, which violate its periodicity. They can be both dynamic fluctuations due to phonons and static ('frozen') fluctuations caused by the violation of the order, for example, due to defects or impurities. The disorder parameter $\Lambda$ is responsible for these fluctuations. In particular, according to [24], absorption for GaAs doped with silicon ($n = 2 \times 10^{18}$ cm$^{-3}$) is greater than that for undoped GaAs; this is obviously caused by the higher $\Lambda$ for doped GaAs due to fluctuations in the spatial distribution of the dopant.

In our case we deal not with a simple compound semiconductor such as GaAs but with solid solutions of two or more semiconductors. Experimental data on this absorption in solid solutions of semiconductors are absent at present. It is believed that in the case of isovalent substitution of some atoms by others (for example, Ga is randomly substituted by Al in AlGaAs solid solution) in typical emitter and barrier layers, the disorder parameter is higher than it could be in doped GaAs samples (see, for example, [24, 25]). The concentration of substituted atoms in typical solid solutions used in semiconductor lasers is several orders of magnitude higher than the dopant concentration. Therefore, the data of papers [24, 25] can be treated as the lower limit for long-wavelength absorption in emitter and barrier layers. In accordance with these assumptions and taking into account the data of papers [24, 25] the value of $\Lambda$ in expression (15) was varied from 5 (which corresponds to pure GaAs) to 100 (for comparison, $\Lambda = 35$ corresponds to p-GaAs with the dopant concentration $10^{20}$ cm$^{-3}$ [25]). Other parameters were borrowed from [24] with the correction of the correspondence of the long-wavelength edge of fundamental absorption band to the bandgap width. Therefore,

$$F_6 = \alpha^{\mathrm{cl}}(T) I(x,y,z). \tag{16}$$

Now we can calculate all the thermal sources in (1) by determining preliminary the flux density of light power and concentration of carriers with the help of the solution of the laser problem.

## 4. Laser problem

To calculate the laser regime we assume that laser radiation propagates in the form of two counterpropagating waves of one transverse mode. This, for example, corresponds to the case of a high-power ridge laser [26, 27]. The total spatial distribution of their intensities $I(x,y,z)$ is given by the relation

$$I(x,y,z) = u(x)v(y)[P^+(z) + P^-(z)], \tag{17}$$

where the transverse intensity distributions of the waves are determined by the functions $u(x)$ and $v(x)$ and the power distributions in the waves propagating in the positive and negative directions along the resonator axis $z$ – by the functions $P^+(z)$ and $P^-(z)$, respectively. For the functions $u(x)$ and $v(x)$, we will use the expressions

$$u(x) = \frac{A\exp\left(-\pi x^2/x_{\mathrm{s}}^2\right)}{|x/x_0|^h + 1},$$
$$v(y) = \frac{\exp\left(-\pi y^2/y_{\mathrm{s}}^2\right)}{y_{\mathrm{s}}}, \tag{18}$$

where $x_{\mathrm{s}}$, $x_0$, and $y_{\mathrm{s}}$ are the optical beam widths along the axes $x$ and $y$, respectively; $h$ is the constant exponent. These quantities were determined with the help of the method of least squares by comparing them, using the results of paper [26], both with calculated and experimentally measured distribution functions for typical ridge lasers. The coefficient $A$ is calculated from the normalisation condition $\int u(x)\mathrm{d}x = 1$, at which

$$A = \left\{\int_{-\infty}^{+\infty} \exp\left(-\frac{\pi x^2}{x_{\mathrm{s}}^2}\right)\left[\left(\frac{x}{x_0}\right)^h + 1\right]^{-1}\mathrm{d}x\right\}^{-1}, \tag{19}$$

and represents an effective inverse width of the optical flux in the direction of the $x$ axis. For quantum-well lasers and lasers with the active region width $d < A$, this coefficient is related with the well-known optical confinement factor $\Gamma$ by the expression

$$A \approx \Gamma/d. \tag{20}$$

The carrier concentration also has a Gaussian transverse distribution

$$N(y,z) = n(z)\exp\left(-\frac{\pi y^2}{w^2}\right), \tag{21}$$

where $w$ is the ridge width. Optical gain in the active layer is given in the linearised form by the relation

$$g = \sigma(T)[N - n_0(T)]. \tag{22}$$

Here, $\sigma(T) = \sigma_0 \exp[-(T - \tilde{T})/T_\sigma]$ is the stimulated emission cross section (differential gain); $n_0(T) = n_0 \times \exp[(T - \tilde{T})/T_N]$ is the density at which the medium becomes transparent (below, transparency density); $T_\sigma$

and $T_N$ are the characteristic temperatures. By introducing the notation

$$T_0^{-1} = T_N^{-1} - T_\sigma^{-1} > 0, \tag{23}$$

where $T_0$ is the characteristic temperature for the threshold current, we will rewrite (22) in the form

$$g = \sigma_0 N \exp\left(-\frac{T-\tilde{T}}{T_\sigma}\right) - \sigma_0 n_0 \exp\left(\frac{T-\tilde{T}}{T_0}\right). \tag{24}$$

Note that because in the model under study the transverse intensity distributions of radiation and carriers are fixed, only the longitudinal distributions $P^+(z)$, $P^-(z)$, and $n(z)$ will be searched for functions of the laser problem. First, these functions specify the sources for the solution of the thermal problem; second, they allow one to find the output laser power. These functions can be found by using laser equations for the intensity and carrier balance described in detail in the second part of this paper. The method for solving the thermal and laser problems and the obtained results are also presented in the second part of the paper.

## 5. Discussion of the model. Conclusions

The specific character of the physical COD model consists in its multifactor structure. Optical damage of the resonator material (output facet) is the result of simultaneous action of many physical processes: absorption of laser radiation due to different mechanisms, propagation of heat in the resonator volume, carrier recombination, etc.

It may appear that from all the possible thermal mechanisms it is sufficient to single out one, the most efficient, and make this mechanism responsible for the COD and consider other mechanisms as some correction or perturbing factors. However, it is clear that from the practical point of view, the COD theory is needed, first of all, to search for new ways to increase its threshold. By eliminating the 'main' mechanism of the COD and thus increasing its threshold, we introduce the next mechanism of importance, after elimination of which, there appears a new one, etc. Therefore, it is very important that the COD theory included as many physical mechanisms participating in this processes as possible. In addition, allowance for many factors affecting the COD in this model allows one to elucidate the role of some specific mechanism by varying the corresponding parameters and thus to formulate the requirements to the parameters of the working medium of a laser (for example, the nonradiative recombination rate, absorption in cladding layers, etc.) in order to ensure its reliable operation. It is for these reasons that the construction of the physical COD model is an urgent separate problem. Our vision of this problem served as the basis for this work.

Another specific feature of the COD consists in the fact that all the mechanisms participating in this process are poorly controlled during the experiment. As a rule, only the final result is obvious, i.e., destruction of the facet; in this case, the experiment with the damaged sample cannot be repeated. This gives rise to additional difficulties when analysing the COD. In this respect, obvious is the advantage of the proposed model, which makes it possible to obtain calculated data characterising the effects preceding the COD. They can be used as some indicator pointing out how large the safety margin of the laser is, i.e., how much the COD threshold exceeds the working power level, and thus to characterise the operation reliability of the laser. Such an indicator is, for example, the temperature rise of the output facet of the laser when its power or operation time increase. Thus, the COD can be predicted long before its appearance.

It may appear that the weak point of the model is the uncertainty of some material parameters characterising the laser medium, because of which they are used in this model as varying quantities. However, from our point of view, this is an objective circumstance. It results from the fact that all these parameters are not absolute constants whose values are specified from the 'first physical principles' but, on the contrary, can change from laser to laser. For example, such parameters as the surface recombination velocity, optical absorption in the degraded layer $\alpha_0^{\text{deg}}$ and its thickness $z_0$ as well as absorption in emitters depend on the manufacturing technology of the laser and their values can indicate the quality of some batch of lasers fabricated by using the same technology.

The model makes use of a simplified quasi-three-dimensional laser problem. The physical justification of this simplification is the fact that transverse (with respect to the laser resonator axis) spatial temperature variations are smoother than transverse variations of the light flux intensity. Therefore, in this model we neglect the effect of temperature variation on the transverse intensity distribution. This is undoubtedly valid for the direction perpendicular to the structure layers and is satisfactorily fulfilled for a ridge laser in the direction along the layers. Note that for a laser with a wide (above 5 μm) active region, this condition is not fulfilled *a fortiori*. From the practical point of view, of particular interest is the COD during the laser operation, when the output parameters of the optical beam are preserved, including the intensity distribution over its cross section. Therefore, the account for the transverse intensity distribution in the beam is hardly reasonable for the COD theory because from the mathematical point of view, its accuracy will most likely exceed the accuracy of the thermal problem and from the practical point of view, it can hardly be very important. Note again that this consideration is not valid for lasers with a wide active region in which the transverse intensity distribution can be change self-consistently as a function of the temperature profile. Finding such intensity and temperature distributions is a separate problem, which is beyond the scope of this work.

***Acknowledgements.*** This work was partially supported by the Educational-Scientific Complex of P.N. Lebedev Physics Institute.

## References

1. Eliseev P.G. *Prog. Quantum Electron.*, **20** (1), 1 (1996).
2. Henry C. H., Petroff P.M., Logan R.A., Merit F.R. *J. Appl. Phys.*, **50** (5), 3721 (1979).
3. Nakwaski W. *J. Appl. Phys.*, **57** (7), 2424 (1985).
4. Nakwaski W. *J. Appl. Phys.*, **67** (4), 1659 (1990).
5. Yoo J.S., Lee H.H., Zory P. *IEEE J. Quantum Electron.*, **28** (3), 635 (1992).
6. Chen G., Tien C.L. *J. Appl. Phys.*, **74** (4), 2167 (1993).
7. Schatz R., Bethea C.G. *J. Appl. Phys.*, **76** (4), 2509 (1994).

8. Hendrix J., Morthier G., Baets R. *IEE Proc. Optoelectron.*, **144** (2), 109 (1997).
9. Menzel U. *Semicond. Science and Technol.*, **13**, 265 (1998).
10. Romo G., Smy T., Walkey D., Reid B. *Microelectron. Reliability*, **43** (1), 99 (2003).
11. Smith W.R. *J. Appl. Phys.*, **87** (12), 8276 (2000).
12. Fukuda M., Okayasu M., Temmyo J., Nakano J. *IEEE J. Quantum Electron.*, **30** (2), 471 (1994).
13. Puchert R., Tomm J.W., Jaeger A., Barwolf A., Luft J., Spath W. *Appl. Phys. A*, **66**, 483 (1998).
14. Gao W., Cheng Z., Xu. L., Luo X., Mastovito A., Shen K. *Proc. SPIE Int. Soc. Opt. Eng.*, **6456**, OB1 (2007).
15. Adachi S. (Ed.) *Properties of Aluminium Gallium Arsenide* (London: INSPEC, 1993) p. 48.
16. Dubey K.S. *J. Thermal Analysis*, **14**, 213 (1978).
17. Adachi S. (Ed.) *Properties of Aluminium Gallium Arsenide* (London: INSPEC, 1993) p. 80.
18. Tansu N., Chang Y.-L., Takeuchi T., Bour D.P., Corzine S.W., Tan M.R., Mawst L.J. *IEEE J. Quantum Electron.*, **38** (6), 640 (2002).
19. Pankove J.I. *IEEE J. Quantum Electron.*, **4** (4), 119 (1968).
20. Snyder C.W., Lee J.W., Hull R., Logan R.A. *Appl. Phys. Lett.*, **67** (4), 488 (1995).
21. Hoffman C.A., Gerritsen H.J., Nurmikko A.V. *J. Appl. Phys.*, **51** (3), 1603 (1980).
22. Ziegler M., Talalaev V., Tomm J.W., Elsaesser T., Ressel P., Sumpf B., Erbert G. *Appl. Phys. Lett.*, **92**, 203506-1 (2008).
23. Agranovich V.M. *Teoriya eksitonov* (Theory of Excitons) (Moscow: Nauka, 1968) p. 152.
24. Johnson S.R., Tiedje T. *J. Appl. Phys.*, **78** (9), 5609 (1995).
25. Pankove J.I. *Phys. Rev.*, **140** (6A), A2059 (1965).
26. Popovichev V.V., Davydova E.I., Marmalyuk A.A., Simakov A.V., Uspenskii M.B., Chel'nyi A.A., Bogatov A.P., Drakin A.E., Plisyuk S.A., Stratonnikov A.A. *Kvantovaya Elektron.*, **32** (12), 1099 (2002) [*Quantum Electron.*, **32** (12), 1099 (2002)].
27. Plisyuk S.A., Batrak D.V., Drakin A.E., Bogatov A.P. *Kvantovaya Elektron.*, **36** (11), 1058 (2006) [*Quantum Electron.*, **36** (11), 1058 (2006)].